

Identification of Two Clinical Hepatocellular Carcinoma Patient Phenotypes From Results of Standard Screening Parameters

Brian I. Carr,^a Petr Pancoska,^b Edoardo G. Giannini,^c Fabio Farinati,^d Francesca Ciccarese,^e Gian Ludovico Rapaccini,^f Maria Di Marco,^g Luisa Benvegnù,^h Marco Zoli,ⁱ Franco Borzio,^j Eugenio Caturelli,^k Maria Chiaramonte,^l Franco Trevisani,^m, for the Italian Liver Cancer (ITA.LI.CA) Group¹

Previous work has shown that two general processes contribute to hepatocellular cancer (HCC) prognosis: liver damage, monitored by indices such as blood bilirubin, prothrombin time (PT), and aspartate aminotransferase (AST); and tumor biology, monitored by indices such as tumor size, tumor number, presence of portal vein thrombosis (PVT) and blood alpha-fetoprotein (AFP) levels. These processes may affect one another, with prognostically significant interactions between multiple tumor and host parameters. These interactions form a context that provide personalization of the prognostic meaning of these factors for every patient. Thus, a given level of bilirubin or tumor diameter might have a different significance in different personal contexts. We previously applied network phenotyping strategy (NPS) to characterize interactions between liver function indices of Asian HCC patients and recognized two clinical phenotypes, S and L, differing in tumor size and tumor nodule numbers. Our aim was to validate the applicability of the NPS-based HCC S/L classification on an independent European HCC cohort, for which survival information was additionally available. Four sets of peripheral blood parameters, including AFP–platelets, derived from routine blood parameter levels and tumor indices from the ITA.LI.CA database, were analyzed using NPS, a graph-theory–based approach that compares personal patterns of complete relationships between clinical data values to reference patterns with significant association to disease outcomes. Without reference to the actual tumor sizes, patients were classified by NPS into two subgroups with S and L phenotypes. These two phenotypes were recognized using solely the HCC screening test results, consisting of eight common blood parameters, paired by their

^aDepartment of Liver Tumor Biology IRCCS de Bellis, National Institute for Digestive Diseases, Castellana Grotte, Italy.

^bCenter for Craniofacial and Dental Genetics, University of Pittsburgh, Pittsburgh, PA.

^cDepartment of Internal Medicine, Gastroenterology Unit, University of Genoa, Genoa, Italy.

^dDepartment of Surgical Science and Gastroenterology, Gastroenterology Unit, University of Padua, Padua, Italy.

^eDivision of Surgery, Policlinico San Marco, Zingonia, Italy.

^fInternal Medicine and Gastroenterology Unit, Catholic University of Rome, Rome, Italy.

^gDivision of Medicine, Azienda Ospedaliera Bolognini, Seriate, Italy.

^hDepartment of Clinical and Experimental Medicine, Medical Unit, University of Padua, Padua, Italy.

ⁱDepartment of Medical and Surgical Science, Internal Medicine Unit, Alma Mater Studiorum – University of Bologna, Bologna, Italy.

^jDepartment of Medicine, Internal Medicine and Hepatology Unit, Ospedale Fatebenefratelli, Milan, Italy.

^kGastroenterology Unit, Ospedale Belcolle, Viterbo, Italy.

^lGastroenterology Unit, Ospedale Sacro Cuore Don Calabria, Negrar, Italy.

^mDepartment of Medical Surgical Sciences, Medical Semiotics Unit, Alma Mater Studiorum – University of Bologna, Bologna, Italy.

¹ These authors contributed equally.

Conflicts of interest: none.

Grant support: ERZ-CZ LL1201 (CORES) to P.P. and NIH grant no. CA 82723 to B.I.C.

Address correspondence to: Brian I. Carr MD, FRCP, PhD, IRCCS ‘S. de Bellis’, via Turi 27, 70013 Castellana Grotte (BA), Italy. E-mail: brianicarr@hotmail.com

0093-7754/- see front matter

© 2014 Elsevier Inc. All rights reserved.

<http://dx.doi.org/10.1053/j.seminoncol.2014.04.002>

significant correlations, including an AFP–platelets relationship. These trends were combined with patient age, gender, and self-reported alcoholism into NPS personal patient profiles. We subsequently validated (using actual scan data) that patients in L phenotype group had $1.5\times$ larger mean tumor masses relative to S, $P = 6 \times 10^{-16}$. Importantly, with the new data, liver test pattern-identified S-phenotype patients had typically $1.7\times$ longer survival compared to L-phenotype patients. NPS integrated the liver, tumor, and basic demographic factors. Cirrhosis-associated thrombocytopenia was typical for smaller S tumors. In L tumor phenotype, typical platelet levels increased with the tumor mass. Hepatic inflammation and tumor factors contributed to more aggressive L tumors, with parenchymal destruction and shorter survival. NPS provides integrative interpretation for HCC behavior, identifying two tumor and survival phenotypes by clinical parameter patterns. The NPS classifier is provided as an Excel tool. The NPS system shows the importance of considering each tumor marker and parameter in the total context of all the other parameters of an individual patient. *Semin Oncol* 41:406-414 © 2014 Elsevier Inc. All rights reserved.

Previous work has shown that two general processes contribute to HCC prognosis. They are liver damage, monitored by indices such as bilirubin, prothrombin time (PT), and aspartate aminotransferase (AST), as well as tumor biology, monitored by indices such as tumor size, tumor number, presence of portal vein thrombosis (PVT) and blood alpha-fetoprotein (AFP) levels.^{1–5} These two general processes may affect one another.^{6–8} Non-disease factors such as gender and age also can influence HCC outcomes,^{9,10} suggesting that any individual disease parameter needs to be considered within a total personal clinical context. Prognostically significant factors may actually function in part through interaction with multiple other tumor and host parameters, as the basis for this context. This context might even provide personalization of the prognostic meaning of these factors for every patient, given his/her individual pattern of measured parameters. Thus, a given level of bilirubin or tumor diameter might have a different significance in different total clinical personal contexts.

We thus considered the levels of standard liver function parameters and commonly assessed tumor indices as part of a pattern, permitting quantification of the impact of the total context of the relationships between all of the parameters combined, on the characterization of the HCC for individual patients. The net result, obtained using a large cohort of Chinese HCC patients in Taiwan ($n = 4,139$) in a training set, was that individual patient parameter relationships between the results of standard blood-based liver tests, which are relevant for prognosis of the HCC outcome were actually not so complex. The relevant information was captured in just nine relationship patterns.¹¹ Important insights into the clinical significance of these nine relationship patterns were revealed, when similarity of each individual patient's patterns to those nine was quantified. The patient profiles exhibited clear heterogeneity: clinical profile patterns of one subgroup were distinctly similar to four, whereas those of other subgroup were similar to

five of those nine “landmark” patterns (we call these important and clinically significant patterns, the heterogeneity landmarks, HLs). Importantly, closeness or distance from these two landmark sets was associated with significantly different tumor masses. We therefore called these two phenotype subgroups of HCC patients with different clinical characteristics S and L, for “exhibiting small” and “exhibiting large” tumor mass, or S- and L-tumor phenotypes for short. It is emphasized that the classification of a patient as having S- or L-tumor phenotype does not include any information about the tumor size and number of tumor nodules. Our pattern-based tumor phenotype identification is based solely on the result of standard blood liver tests, including those for hepatitis, as well as the presence or absence of PVT, and basic demographic information (gender, age, alcohol history). Here, we present further insights into the clinical relevance of pattern based characterization of HCC. In the Taiwan study, survival data were not available. In the current reprot, we have used a database of 2,773 HCC patients with known survival outcomes. There were two main goals of processing these independently collected Italian test data through the same diagnostic scheme, which was developed in the training data set. The first was to validate that these two characteristic pattern sets of blood-based liver test results and personalized characterization of the closeness and differences from these clinical patterns will identify the same S- and L-tumor phenotypes. The second goal was to show that blood-test pattern-based identification of the S- and L-tumor phenotypes also identifies patients with significantly different survival outcomes.

METHODS

Data Collection

We retrospectively analyzed prospectively-collected data in the Italian Liver Cancer (ITA.LI.CA) database of HCC patients accrued at 11 centers.¹²

Newly diagnosed HCC patients (2,773 in all) had full baseline parameter data, including radiology of maximum tumor diameter (MTD), number of tumor nodules, and presence of PVT; demographics (gender, age, alcohol history, presence of hepatitis B or C); blood counts (hemoglobin, white blood cells, platelets, prothrombin time); blood AFP and routine liver function tests (total bilirubin, AST, alkaline phosphatase [ALKP], gamma glutamyltranspeptidase [GGTP], albumin). I.T.A. LI.CA database management conforms to Italian legislation on privacy and this study conforms to the ethical guidelines of the Declaration of Helsinki. Approval for the study on de-identified patients was obtained by the Institutional Review Board of participating centers.

Data Processing

The clinical parameter data were processed exactly as previously.^{11,13} These primary data were pre-processed in the same way as the training set. Concretely, we first performed analysis of complete set of all pairwise correlations between these data and confirmed (using the representation of the full correlation matrix as a complete weighted graph and identifying the maximal cut in this graph) that in the Italian data the same optimal pairing of the variables as in the previous study was found. Thus, the blood counts and routine liver function test variables were grouped into AST/alanine aminotransferase (ALT), albumin/hemoglobin, bilirubin/international normalized ratio (INR) and platelet–AFP pairs, that had, as in the training set, the unique property that all these pairs were statistically significantly correlated and, simultaneously, the sum of their pairwise correlation coefficients was the largest of all other alternative pairings and groupings possible. In the next methodology validation step, we independently confirmed that the two variable thresholds for each of these four blood test pairs, which we derived by the tertile-based training set processing, also subdivided this test cohort into subgroups consisting of one tertile of patients with the highest paired parameter levels (high-level subgroup) and two tertiles of patients (low-level subgroup) with the lower levels of the paired parameters. After these details of the data pre-processing steps were independently validated, we converted all patients' raw data into the high- and low-blood test subgroups. By adding the remaining information, we constructed the personal relationship pattern (PRP_i) for each individual patient (see [Figure S1, Appendix](#)). This was followed by computing the edit-distance δ_k (PRP,HL[k]) between these PRPs and the nine landmark patterns HL[1], HL[2], ..., HL[9], determined by the NPS processing of the training set. As the result, the clinical status of each patient, explicitly incorporating the information concerning the individual clinical context pattern, was represented by a series of nine

values of δ_k . These nine values were entered as input variables into the logistic regression equation, which was previously optimized using the training set, to compute the odds for classification of every individual patient as having S- or L-tumor phenotype. We did not re-optimize either the set of nine HLs or the coefficients of the diagnostic logistic regression equation. We used this blood liver test plus demographic based identification of the two patient subgroups (one with higher odds for S-, the other with higher odds for L-tumor phenotype) in all subsequent validation and interpretive steps discussed here. The data processing summary and parameter–relationship pattern-based classification model is shown in [Figure S1 \(Appendix\)](#).

RESULTS

Independent Validation of S and L Clinical Phenotyping

[Figure 1a](#) shows box plots of the distributions of the tumor masses for patients from the Italian test set, recognized by the odds computed from the differences of their standard screening result personal relationship patterns from the nine HLs as having the S- and L-tumor phenotypes. The means of these distributions were significantly different, $P = 6 \times 10^{-16}$. The statistical significance as well as the mean differences of the tumor mass distributions of this outcome of the two standard screening identified HCC groups are comparable to the tumor mass differences between these two HCC tumor phenotypes, identified by our relationship pattern analysis in the Chinese patient training dataset.

Although the difference of means was highly statistically significant, there was still significant overlap in the distributions of the tumor masses in the two groups. The overlap reflects the complexity of the HCC phenotype together with the unknown point on the course of the HCC development at the point of any individual patient diagnosis. Nevertheless, having the complete patient cohort independently subdivided into two subgroups with markedly different clinical patterns allowed identifying S- and L-phenotype subgroups, which was not possible by analyzing the complete cohort. Applying the Kaplan-Meier statistics to these two independently recognized groups, we found that probability of finding the same tumor mass in the S- and L-tumor phenotype HCC groups was significantly different ([Figure 1c](#), differences between the probabilities are larger than $2 \times 95\%$ confidence interval of the respective probability estimates).

Survival was also analyzed in two ways. First, we tested the statistical significance of the differences in means of the survival distributions, computed separately for the two groups, identified from the results of their standard screening tests as S- and L-tumor

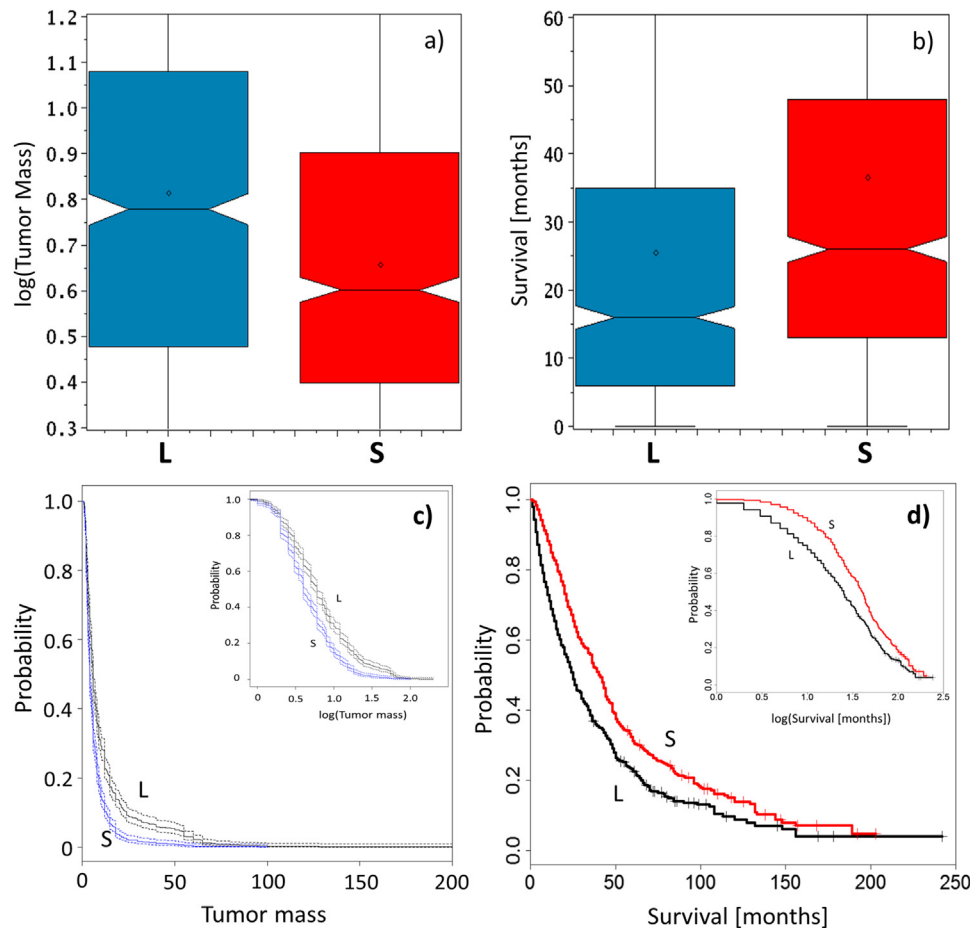


Figure 1. Validation of HCC outcome differences for patients with S- and L-tumor phenotypes, identified by NPS analysis of standard screening results. Boxplots of the differences in the a) tumor masses and b) in the overall survival for patients with the S- and L-tumor phenotypes. Kaplan-Meier plots of the significant differences between the probabilities to find equivalent c) tumor masses and d) overall survivals for patients with the S and L-tumor phenotypes.

phenotype patients (see box plots, [Figure 1b](#)). The mean overall survival for S-tumor phenotype patients was 24 months, whereas it was 14 months for L-tumor phenotype patients (difference statistically significant, $P = 10^{-21}$). Thus, S-tumor phenotype patients had 1.7 times longer mean survival compared to L-tumor phenotype patients. Second, we performed Kaplan-Meier survival analysis, based on the standard-screen results NPS identification of the S- and L-tumor phenotype patients and found significantly different probabilities of survival in these S and L HCC tumor phenotype patient subgroups (see [Figure 2d](#)). The typical separation of the S- and L-tumor phenotype survival probability curves is statistically significant, exceeding twice the 95% confidence interval of the two estimated survival probabilities.

Tumor Mass Relationships in S- and L-Tumor Phenotype Groups

The identification of S- and L-tumor phenotype subgroups, differing in survival, resulted from the

analysis of relationship patterns between indices of liver function, which independently provided the significantly different tumor and survival parameters. This provides the basis for analysis of functional differences between the two phenotypes, because we can now separately analyze patients from the two well-defined phenotypic groups. To visualize dominant trends in relationships between the screening and outcome clinical variables, a moving average processing of biologically interesting parameter pairs was used. In the first part of this analysis step, the relationships between clinical parameters and tumor mass were inspected. Patients were first ordered according to tumor mass, separately in S- and L-tumor phenotype groups and then the clinical parameter and tumor mass values were processed by the moving average to reveal dominant trends between the data in the pair. The relationships between tumor mass and both internal tumor factors (AFP) and liver function factors (bilirubin, AST, GGTP) were studied. [Figure 2a](#) shows that the typical trends between bilirubin and tumor mass are

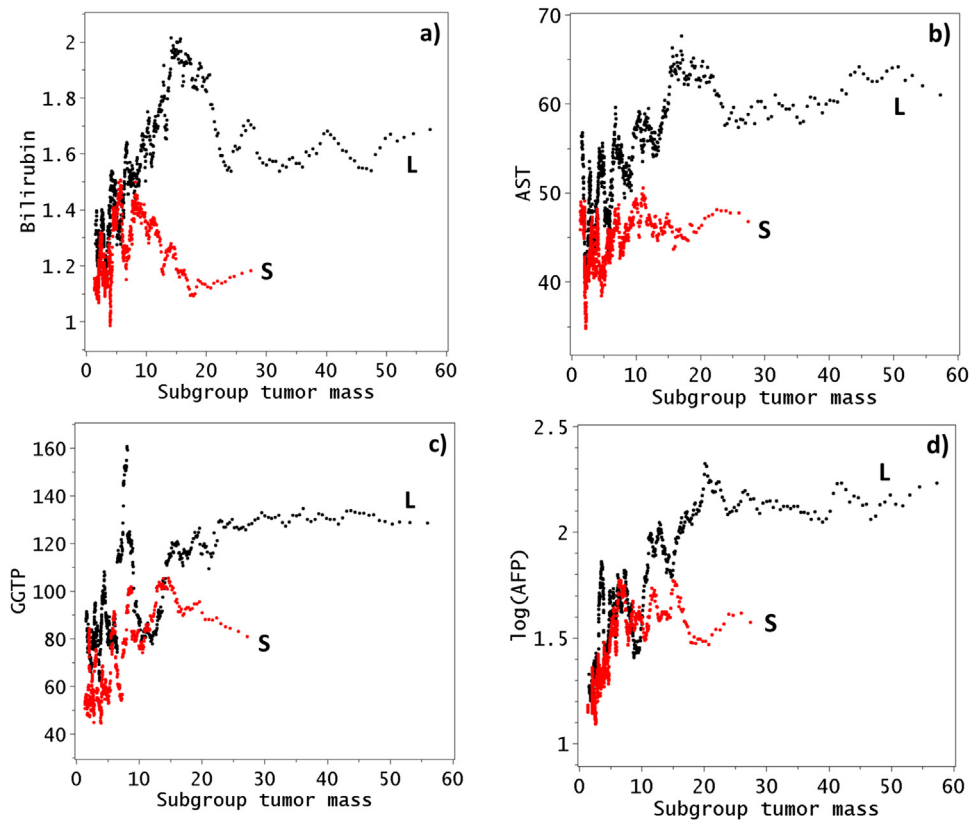


Figure 2. Trends between typical values of tumor masses and various clinical parameters as they differ for S- and L-tumor phenotypes, identified via NPS from standard screening results.

different between S- and L-tumor phenotypes. Overall, there were higher typical bilirubin levels in S-tumor phenotype subgroup than in L, for a given tumor mass. For both groups, bilirubin increased with increasing mass for smaller tumors. However, with additional increases in tumor mass, there appeared to be no further relationship between increasing mass and bilirubin levels, accompanied by a lowering of typical bilirubin levels. This transition in the relationship between mass and bilirubin occurred at smaller tumor masses in S compared with L tumors. This lack of further increase in bilirubin levels as the tumors continued to grow, suggested to us that beyond a certain mass, factors internal to the tumor were dominant in the increasing tumor growth. This looks like a plausible functional hypothesis, but evidence from just one (bilirubin) clinical variable is insufficient. The novelty of our characterization of S and L HCC tumor phenotypes is in recognizing them from the differences in the clinical data relationship patterns in the two groups, instead of from the conventional normal/elevated clinical variable level approach. Thus, any functional interpretation of what is observed for a single clinical variable in relationship to the tumor characteristic or disease outcome has to be contrasted and confirmed by examining the trends in other liver parameters. Following these ideas, we therefore examined trends

revealed by the moving-average processing for AST and GGTP with respect to increasing tumor mass. They showed remarkable similarities to the trends for bilirubin (Figures 2b and 2c).

These results also showed that beyond a certain small tumor mass, continued tumor growth was not accompanied by increased evidence for tumor damage. In this multi-variable context, it is interesting that the examination of AFP trends showed increased levels with increasing tumor mass and were comparable for both S- and L-tumor phenotype groups. AFP thus appears to monitor tumor growth through its full range, unlike the changes in liver function parameters (Figure 2d). Another observation was that beyond a certain point of tumor growth, further increase in tumor mass was associated with a lesser increase in AFP per unit increase in tumor mass. This change in the slope in the relationship of the tumor mass–AFP trend occurred at the same tumor mass that marks the decrease in related trends for both bilirubin and AST. All of these results, combined and interpreted in a mutual context, are consistent with the hypothesis that, with further tumor growth, the contribution from liver factors decreased while the internal tumor factors linked to growth increased, as reflected in the lesser response of AFP to further increases in tumor mass. An analysis was done for trends of liver function parameters for increasing AFP

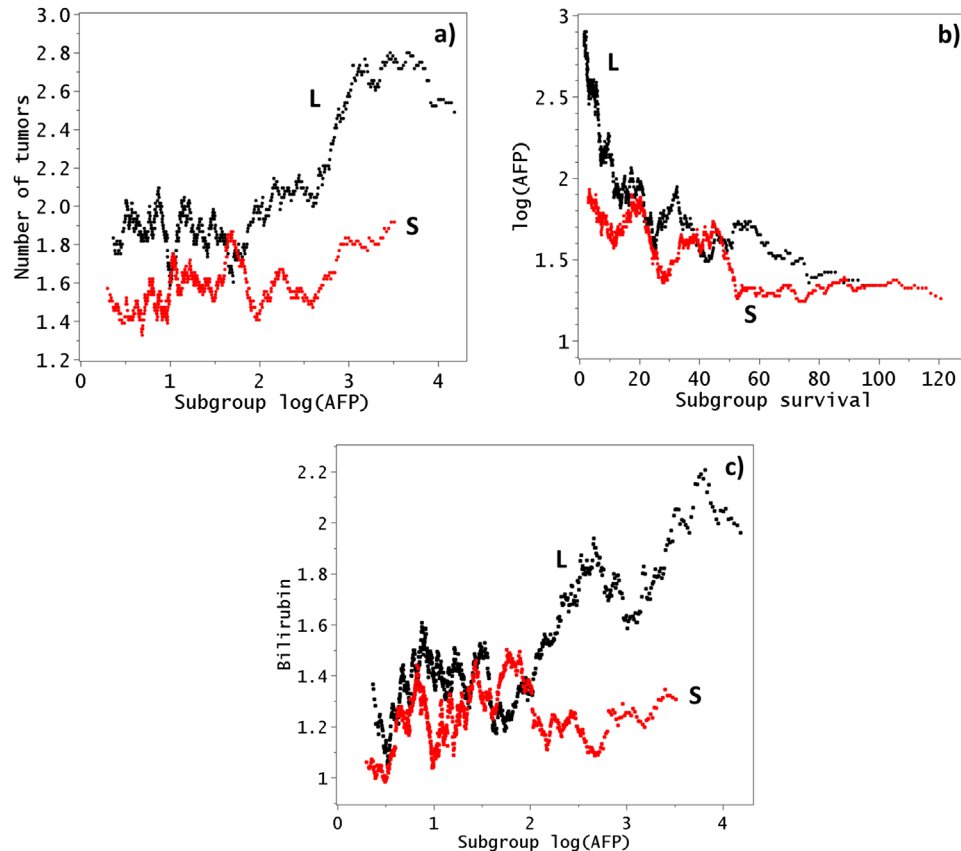


Figure 3. Trends between typical values of AFP levels in log-scale and a) tumor numbers, b) survival, and c) bilirubin, as they differ for S- and L-tumor phenotypes, identified via NPS from standard screening results.

instead of increasing tumor mass. The results were very similar (data not shown).

AFP Relationships

Given the finding of AFP as a monitor of HCC growth, reported above, we next analyzed the typical levels of liver function parameters for patients with comparable AFP levels, separately for S- and L-tumor phenotype groups. We analyzed patterns in bilirubin, tumor numbers and survival with respect to AFP levels (Figure 3). We found that the number of tumors increased with increasing AFP levels in both phenotypes. However, there were typically a smaller number of tumors in S- compared with L-tumor phenotype, for patients with comparable AFP levels (Figure 3a). Furthermore, beyond AFP 300 ng/mL levels (~ 2.5 in log-scale), tumor numbers increased at a greater rate in L patients than in S patients. Thus, the increase in tumor mass from AFP 1–300 ng/mL (0- to 2.5-log scale, depicted in Figure 2) is likely due to increase in tumor size alone, but above this AFP threshold, the increase in tumor mass also has a contribution from increased number of tumor nodules, mainly in the L-tumor phenotype group. The increase in numbers of

tumors in S-tumor phenotype group was only modest. Increasing AFP levels were associated with decreasing survival. Thus, for a given similarity of survival, L-tumor patients had higher AFP than S-tumor phenotype patients (Figure 3b). Given the importance of both liver and tumor factors, we next plotted the trends in bilirubin levels as a function of increasing AFP levels. We found incoherency between bilirubin and typical AFP levels up to log AFP 100 ng/mL (2 in log-scale). Thereafter, this trend continued for S-tumor phenotype patients, but not L, in whom increasing AFP was followed by increasing bilirubin levels (Figure 3c). In Figure 2a, increase in tumor mass was not associated with increase in bilirubin levels in S-tumor phenotype patients. This transition in AFP levels to approximately 100 ng/mL corresponds to the change in the rate of increase per unit of tumor mass and also to the point at which bilirubin/tumor mass level changes diverged between S- and L-tumor phenotype in Figure 2.

Platelet Relationships

Our initial analysis of complete correlations between all parameters (Methods) showed that platelets and AFP were part of the set of four pairs

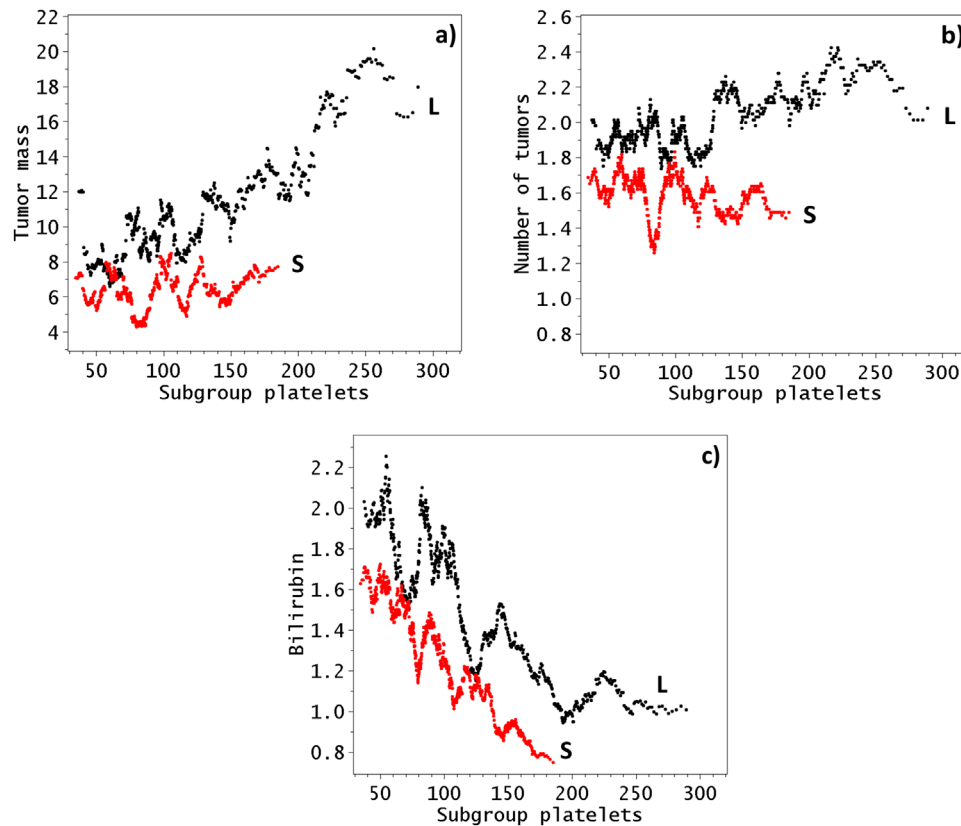


Figure 4. Trends between typical values of platelet levels and a) tumor mass, b) tumor numbers, and c) bilirubin as they differ for S- and L-tumor phenotypes, identified via NPS from standard screening results.

with the highest correlations. Patterns of trends between platelets and other parameter were next examined and no correlation of platelet counts with tumor mass or tumor number for S-tumor phenotype patients (Figure 4). Conversely, there was a linear trend between typical platelet values and tumor mass or number of nodules for L-tumor phenotype patients (Figures 4a and 4b). In addition, platelet counts were systematically lower in S- than L-tumor phenotype patients. In both S- and L-tumor phenotype patients, the platelets decreased with increased bilirubin levels, consistent with the inverse bilirubin/platelet relationship of liver failure.

DISCUSSION

We previously used a network phenotyping strategy (NPS) on a large cohort of Chinese HCC patients to show that analysis of standard screening parameter relationship patterns could identify two sets of HCC patient phenotypes, called S- and L-tumor phenotype groups.¹¹ The results showed that if the individual parameter values were considered in the context of all other parameters, we could identify independently two possible sets of tumor phenotypic patterns. Survival data was not available for that analysis. Therefore, we have now extended the

clinical meaning of that initial study, by examining whether this approach could be used to examine a large and completely different HCC cohort in another ethnic patient HCC group, using the identical method of standard screening data processing and the same quantitative NPS model and by assessing our HCC phenotyping model on survival. We found that our previous results were replicated; specifically the total cohort studied here could be again clearly separated into S- and L-tumor phenotypes, each associated with significantly different tumor masses and newly also with significantly different survival. Our NPS classification algorithm is made available as user-friendly Excel worksheet (see Appendix, file NPSClassifier.xls).

The main findings of this study include the functional insight into survival factors deduced from independently examined relationships between various standard clinical parameter patterns and total tumor mass (Figures 2 and 3) in the two recognized tumor phenotypes. Three liver function parameter trends in relation to tumor mass showed distinct differences between S- and L-tumor phenotypes: trends for bilirubin, AST, and GGTP showed an increase with increasing tumor mass for L, but not for S patients, beyond a limited tumor mass. However, the trends for AFP were different than for AST,

GGTP, and bilirubin, since there was a general non-linear increase in AFP with tumor mass for both S- and L-tumor phenotype patients. We interpret this to signify a close link between AFP production and tumor growth, in both S- and L-tumors. By contrast, we suppose that involvement of bilirubin, AST and GGTP with tumor mass is more indirect. Thus, AFP could be a mediator of internally derived growth of HCCs (oncogenes, growth factors), whether of S- or L-tumor phenotype, whereas liver function parameters might chiefly reflect the tumor microenvironment that permits or modulates HCC growth and behavior. We found that trends for bilirubin, AST and GGTP were all higher for the larger and more aggressive HCC L-phenotype tumors, which also were associated with shorter survival than S-tumor phenotype patients. Therefore, this NPS approach synthesizes and integrates both liver and tumor factors.

The novel NPS analysis was based on the patterns instead of individual parameter values and reveals both characteristic interrelationships between liver function and tumor biology patterns and their manageable complexity in HCC phenotypes. Both liver and tumor factors are previously well-described determinants of HCC prognosis. Our relationship pattern-based processing of the parameter data permitted us to integrate them in a well-characterized NPS scheme, and to discern two distinct clinical HCC tumor phenotypes, in which the relative importance of liver and tumor factors was rather different. Inspecting typical trends between different parameters, we found increasing trends in L-tumor phenotypes for several parameters, but constancy in parameter trends for S-phenotype, which suggests some possible mechanistic interpretations. Most HCCs arise on the basis of hepatic inflammation with some degree of associated cirrhosis,^{14–16} and this background is consistent with elevated bilirubin, AST, and GGTP for both S- and L-tumors. The portal hypertension and splenomegaly associated thrombocytopenia appeared mainly as a feature of patients having S-tumors, reflecting small size HCC development in cirrhosis.¹⁷ As S-tumors grew, they did not appear to further worsen the liver function parameters, possibly due to their significantly smaller size compared to L-tumors. The parameter trends were more complex in L-tumors, likely due to multiple factors, including hepatic inflammation and endogenous tumor factors. Unlike S-tumor phenotype patients, the L-tumor phenotype patients, identified by our NPS processing of screening data, predominantly had less thrombocytopenia. It is tempting to hypothesize that in L-, unlike S-tumor phenotype patients, the platelet-derived tumor growth factors^{18–25} and inflammatory cytokines^{26,27} may play a role in the expansion of the growing tumor mass.

There is an inverse relationship between bilirubin and platelet levels in portal hypertension; our patients were no exception (Figure 4c). However, other causes could also contribute to the higher bilirubin levels associated with large tumors in L-tumors (Figure 2a), including inflammation, parenchymal destruction and biliary invasion by large tumor masses (Figure 2a, b, and c). Thus, beyond a certain small tumor mass, further increases of mass were associated with higher bilirubin levels in L-, but not in S-tumor phenotype patients. According to our results, S- and L-tumor phenotypes differ in the relative contributions of these mechanisms, recognizable by their different patterns. We found that platelets and AFP were one of the set of four parameter pairs with the highest correlations in the total cohort. There was a linear trend between platelet values and both tumor mass or number of nodules for L-tumor mass phenotype patients, but not for S-patients, showing the importance of the platelet-AFP pairing, but also the profound differences between L- and S-phenotype patients.

APPENDIX. SUPPLEMENTARY DATA

Supplementary data associated with this article can be found in the online version, at <http://dx.doi.org/10.1053/j.seminoncol.2014.04.002>.

REFERENCES

1. Qin LX, Tang ZY. The prognostic significance of clinical and pathological features in hepatocellular carcinoma. *World J Gastroenterol.* 2002;8:193–9.
2. Cabibbo G, Maida M, Genco C, et al. Natural history of untreatable hepatocellular carcinoma: a retrospective cohort study. *World J Hepatol.* 2012;4:256–61.
3. Lee YH, Hsu CY, Hsia CY, et al. A prognostic model for patients with hepatocellular carcinoma within the Milan criteria undergoing non-transplant therapies, based on 1106 patients. *Aliment Pharmacol Ther.* 2012;36:551–9.
4. Park KW, Park JW, Choi JI, et al. Survival analysis of 904 patients with hepatocellular carcinoma in a hepatitis B virus-endemic area. *J Gastroenterol Hepatol.* 2008;23:467–73.
5. Cabibbo G, Genco C, Di Marco V, et al. Predicting survival in patients with hepatocellular carcinoma treated by transarterial chemoembolisation. *Aliment Pharmacol Ther.* 2011;34:196–204.
6. Hoshida Y, Villanueva A, Kobayashi M, et al. Gene expression in fixed tissues and outcome in hepatocellular carcinoma. *N Engl J Med.* 2008;359:1995–2004.
7. Leonardi GC, Candido S, Cervello M, et al. The tumor microenvironment in hepatocellular carcinoma (review). *Int J Oncol.* 2012;40:1733–47.
8. Utsunomiya T, Shimada M, Imura S, Morine Y, Ikemoto T, Mori M. Molecular signatures of noncancerous liver tissue can predict the risk for late recurrence of

- hepatocellular carcinoma. *J Gastroenterol.* 2010;45:146-52.
9. Buch SC, Kondragunta V, Branch RA, Carr BI. Gender-based outcomes differences in unresectable hepatocellular carcinoma. *Hepatol Int.* 2008;2:95-101.
 10. Carr BI, Pancoska P, Branch RA. HCC in older patients. *Dig Dis Sci.* 2010;55:3584-90.
 11. Pancoska P, Lu S-N, Carr BI. Phenotypic categorization and profiles of small and large hepatocellular carcinomas. *J Gastrointest Dig Syst.* 2013;S12:001. PMID: 23956952. Epub.
 12. Santi V, Buccione D, Di Micoli A, et al. The changing scenario of hepatocellular carcinoma over the last two decades in Italy. *J. Hepatol.* 2012;56:397-405.
 13. Pancoska P, Carr BI, Branch RA. Network-based analysis of survival for unresectable hepatocellular carcinoma. *Semin Oncol.* 2010;37:170-81.
 14. Della Corte C, Aghemo A, Colombo M. Individualized hepatocellular carcinoma risk: the challenges for designing successful chemoprevention strategies. *World J Gastroenterol.* 2013;19:1359-71.
 15. Karagozian R, Baker E, Houranieh A, Leavitt D, Baffy G. Risk profile of hepatocellular carcinoma reveals dichotomy among US veterans. *J Gastrointest Cancer.* 2013 Apr 23. Epub.
 16. Mittal S, El-Serag HB. Epidemiology of hepatocellular carcinoma: consider the population. *J Clin Gastroenterol.* 2013 Apr 29. Epub.
 17. Carr BI, Guerra V, Pancoska P. Thrombocytopenia in relation to tumor size in patients with hepatocellular carcinoma. *Oncology.* 2012;83:339-45.
 18. Yang ZF, Ho DW, Lau CK, et al. Platelet activation during tumor development, the potential role of BDNF-TrkB autocrine loop. *Biochem Biophys Res Commun.* 2006;346:981-5.
 19. Zhou J, Tang YZ, Fan J, et al. Expression of platelet-derived endothelial cell growth factor and vascular endothelial growth factor in hepatocellular carcinoma and portal vein tumor thrombus. *J Cancer Res Clin Oncol.* 2000;126:57-61.
 20. Stock P, Monga D, Tan X, et al. Platelet-derived growth factor receptor-alpha: a novel therapeutic target in human hepatocellular cancer. *Mol Cancer Ther.* 2007;6:1932-41.
 21. Campbell JS, Hughes SD, Gilbertson DG, et al. Platelet-derived growth factor C induces liver fibrosis, steatosis and hepatocellular carcinoma. *Proc Natl Acad Sci U S A.* 2005;102:3389-94.
 22. Soll C, Jang JH, Riener MD, et al. Serotonin promotes tumor growth in human hepatocellular cancer. *Hepatology.* 2010;51:1244-54.
 23. Gauglhofer C, Sagmeister S, Schrottmaier W, et al. Up-regulation of the fibroblast growth factor 8 subfamily in human hepatocellular carcinoma for cell survival and neoangiogenesis. *Hepatology.* 2011;53:854-64.
 24. Miura S, Mitsuhashi N, Shimizu H, et al. Fibroblast growth factor 19 expression correlates with tumor progression and poorer prognosis of hepatocellular carcinoma. *BMC Cancer.* 2012;12:56.
 25. French DM, Lin BC, Wang M, et al. Targeting FGFR4 inhibits hepatocellular carcinoma in preclinical mouse models. *PLoS One.* 2012;7:e36713.
 26. Sitia G, Aiolfi R, Di Lucia P, et al. Antiplatelet therapy prevents hepatocellular carcinoma and improves survival in a mouse model of chronic hepatitis B. *Proc Natl Acad Sci U S A.* 2012;109:E2165-72.
 27. Spengler U. Hepatic microcirculation: a critical but neglected factor for the outcome of viral hepatitis. *J Hepatol.* 2009;50:631-3.